Intelligent Reflecting Surface-Assisted NLOS Sensing via Tensor Decomposition

Jilin Wang¹, Jun Fang¹, Hongbin Li²

¹University of Electronic Science and Technology of China, Chengdu, China
²Stevens Institute of Technology, Hoboken, USA
jilinwang@std.uestc.edu.cn, JunFang@uestc.edu.cn, Hongbin.Li@stevens.edu

Abstract—We consider the problem of intelligent reflecting surface (IRS) assisted target sensing in a non-line-of-sight (NLOS) scenario, where the line-of-sight (LOS) path between the access point (AP) and the target is blocked by obstacles, and an IRS is employed to facilitate the AP to sense the targets that are distributed in its NLOS region. The AP transmits orthogonal frequency division multiplexing (OFDM) pulses and then perceives the targets based on the echoes from the AP-IRS-targets-IRS-AP link. To resolve an inherent scaling ambiguity for IRSassisted NLOS sensing, we propose a two-phase sensing scheme by exploiting the diversity in the illumination pattern of the IRS across two different phases. Specifically, the received echo signals from the two phases are constructed as two third-order tensors. Then a CANDECOMP/PARAFAC decomposition (CPD)-based method is developed to extract target parameters from the two constructed tensors. Simulation results are provided to show the effectiveness of the proposed method.

Index terms— Intelligent reflecting surface, non-line-ofsight sensing, OFDM, CANDECOMP/PARAFAC decomposition

I. INTRODUCTION

Intelligent reflecting surface (IRS) has received a great amount of attention in wireless communications due to its ability of reconfiguring wireless propagation channels [1]. Specifically, IRS is made of a newly developed metamaterial comprising a large number of reconfigurable passive components. Through a smart controller, the phase and amplitude of each unit on the IRS can be flexibly adjusted. This allows for coherent or destructive addition of reflected signals at the receiver, enabling passive beamforming, increased spectral efficiency, interference suppression, and other benefits [2].

In wireless sensing systems, IRS provides an additional virtual LOS link from the wireless node to the target, which can be leveraged to enhance the sensing performance. When the LOS path from the wireless node to the target is blocked, the AP-IRS-target-IRS-AP link provided by the IRS can be explored for NLOS target sensing [3]. In [4], the authors examined the radar equation for the NLOS scenario and evaluated the sensing performance in terms of signal-to-noise ratio (SNR) and signal-to-clutter ratio (SCR). In [5], an IRS-aided multi-input multi-output (MIMO) radar detection problem was considered, where the IRS phase shifts were optimized to maximize the probability of detection for a fixed probability of false alarm. Furthermore, [6] considered IRS-enabled NLOS sensing problem, which involves utilzing the received echo signal from the AP-IRS-target-IRS-AP link



Fig. 1: System model of IRS-assisted sensing.

to estimate the target's parameter. Additionally, the transmit beamformer at the AP and the reflection beamformer at the IRS were optimized by minimizing the Cramér-Rao bound (CRB) for the considered estimation problem. However, [6] only considered a single target, and it assumed that the rank of AP-IRS channel is greater than one in order to avoid a scaling ambiguity that is inherent in IRS-assisted NLOS sensing. Such an assumption may not be satisfied in practice.

In this paper, we consider an IRS-assisted wireless sensing system, where the LOS path between the AP and the target is blocked by obstacles. The AP transmits a sensing signal and then perceives the targets based on the echo signal from the AP-IRS-targets-IRS-AP link. To resolve the inherent scaling ambiguity, we propose a two-phase sensing method, where the entire sensing cycle consists of two phases, and each phase employs a distinct IRS-phase-shift profile. By utilizing the diversity of the IRS illumination pattern across the two different phases, we develop a CPD-based method that can uniquely identify target parameters even when there is only a single path between the AP and the IRS.

II. PROBLEM FORMULATION

A. System Model

Consider an IRS-assisted wireless sensing (i.e., radar) system, where the LOS path between the radar/access point and the target is blocked by obstacles (see Fig.1). The access point (AP) transmits a sensing signal and then perceives the targets based on the echo signal propagating through the AP-IRS-targets-IRS-AP channel. Suppose the AP is equipped with a uniform linear array (ULA) of M antennas, and the IRS is equipped with a ULA of N reflecting elements. We assume that there are K targets located in the area that are illuminated

by the IRS. Let $\boldsymbol{x}(t) \in \mathbb{C}^M$ denote the transmitted signal, and $\boldsymbol{G} \in \mathbb{C}^{N \times M}$ denote the channel matrix from the AP to the IRS. Each reflecting element of the IRS can independently reflect the incident signal with a reconfigurable phase shift. Define $\vartheta_n \in [0,2\pi]$ as the phase shift associated with the nth reflecting element of the IRS. Also, define the phase shift matrix of the IRS as

$$\mathbf{\Phi} = \operatorname{diag}(e^{j\vartheta_1}, \cdots, e^{j\vartheta_n}) \in \mathbb{C}^{N \times N} \tag{1}$$

Let θ denote a target's direction-of-arrival (DOA) with respect to the IRS. The corresponding steering vector at the IRS can be written as

$$\boldsymbol{a}(\theta) = \frac{1}{\sqrt{N}} [1 \ e^{j2\pi \frac{d\sin(\theta)}{\lambda}} \ \cdots \ e^{j2\pi \frac{(N-1)d\sin(\theta)}{\lambda}}]^T \quad (2)$$

where d denotes the spacing between any two adjacent reflection elements, and λ is the wavelength of the carrier signal. For the kth target, the cascaded IRS-target-IRS channel can be written as

$$\boldsymbol{H}_k = \tilde{\alpha}_k \boldsymbol{a}(\theta_k) \boldsymbol{a}^T(\theta_k) \tag{3}$$

where $\tilde{\alpha}_k \in \mathbb{C}$ is used to characterize the round-trip path loss as well as the radar cross section (RCS) coefficient of the kth target. Define $\boldsymbol{H} \triangleq \sum_{k=1}^K \boldsymbol{H}_k$. In this paper, we assume that there is only a single dominant path between the AP and the IRS, i.e., $\mathrm{rank}(\boldsymbol{G}) = 1$, which is usually the case for many practical scenarios. In fact, as pointed out in [6], under such a circumstance, the target's DOA parameter cannot be uniquely identified due to inherent scaling ambiguities. To ensure the identifiability of the DOA parameter, the work [6] requires the rank of the channel matrix \boldsymbol{G} to be greater than 1. Such a condition, however, may not be met in practice. In this work, we propose a two-phase sensing method which is able to identify targets' DOA parameters even for rank-1 channel \boldsymbol{G} by exploiting the IRS's illumination pattern diversity in two different phases.

B. Received Signal Model

In a coherent processing interval (CPI), the AP transmits a train of P uniformly-spaced OFDM pulses. In each pulse, the AP transmits one OFDM block and then receives the echo form potential targets. Suppose there are L orthogonal subcarriers in each block and the subcarrier spacing is set as $\Delta f = 1/T_{\rm d}$. The duration of one block is $T = T_{\rm cp} + T_{\rm d}$, where $T_{\rm cp}$ is the length of the cyclic prefix (CP) and $T_{\rm d}$ is the duration of an OFDM symbol. Define $T_{\rm PRI}$ as the pulse repetition interval (PRI). The baseband signal in the pth pulse can be expressed as

$$s_p(t) = \sum_{l=1}^{L} \beta_l e^{j2\pi l\Delta f t} \xi(t - pT_{\text{PRI}})$$
 (4)

where $pT_{\text{PRI}} \leq t \leq pT_{\text{PRI}} + T$, $\xi(t)$ is the rectangular function that takes 1 for $t \in [0,T]$ and 0 otherwise [7], and β_l is the unit-energy modulated symbol which satisfies $|\beta_l|^2 = 1, \forall l$. For such a signal, it can be readily verified that the CP is a repetition of the end part of the OFDM block for any $T_{\text{cp}} = \mu T, 1 > \mu > 0$. Also, for simplicity, we assume

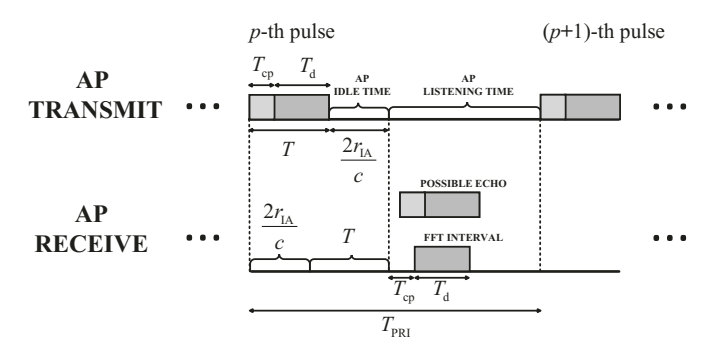


Fig. 2: A schematic of signal transmission in one pulse repetition interval.

 $\beta_l = \beta, \forall l$ in this paper. Suppose we use a distinct transmit beamforming vector $\boldsymbol{w}_p \in \mathbb{C}^M$ to transmit the pth pulse. Then the transmitted signal can be expressed as

$$\boldsymbol{x}_p(t) = \sqrt{P_t} \boldsymbol{w}_p s_p(t) \exp(j2\pi f_c t)$$
 (5)

where P_t denotes the transmit power and f_c denotes the carrier frequency. Assume that the kth target is located at a distance of R_k (m) from the IRS and the target is moving towards the IRS with a radial velocity of v_k (m/s). After transmitting the pth pulse, the AP starts to listen to its echo signal after a duration of $2r_{\rm IA}/c$ seconds, where c denotes the speed of light and $r_{\rm IA}$ denotes the distance between the AP and the IRS. Such a duration is used as a guard interval to avoid the interference signal directly reflected from the IRS (see Fig.2). Also, we make the following assumption in order to acquire the complete echo signal reflected from the targets.

Assumption 1 The echo signals from all potential targets are assumed to lie within the interval of $[2r_{IA}/c+T, 2r_{IA}/c+2T+T_{cp}]$.

To process the received signal, a Fourier transform operation is performed over the interval $[2r_{\rm IA}/c+T+T_{\rm cp},2r_{\rm IA}/c+2T]$. When Assumption 1 is satisfied, it means that the earliest possible echo signal reflected by a potential target will be received over the interval $[2r_{\rm IA}/c+T,2r_{\rm IA}/c+2T]$, and the latest possible echo signal reflected by a potential target will be received within the interval $[2r_{\rm IA}/c+T+T_{\rm cp},2r_{\rm IA}/c+2T+T_{\rm cp}]$. Since the CP part is the repetition of the end part of the OFDM block, the interval $[2r_{\rm IA}/c+T+T_{\rm cp},2r_{\rm IA}/c+2T]$ contains each target's complete echo signal.

Since the AP operates in a listening mode within the interval $[2r_{\rm IA}/c + T, T_{\rm PRI}]$, the received echo signal only contains signals reflected by targets. Thus, for the pth pulse, the received signal at the mth antenna of the AP can be written as

$$\tilde{y}_{p,m}(t) = \sum_{k=1}^{K} \boldsymbol{g}_{m}^{T} \boldsymbol{\Phi}^{T} \boldsymbol{H}_{k} \boldsymbol{\Phi} \boldsymbol{G} \boldsymbol{x}_{p}(t - \tau_{p,k}) + \tilde{n}_{p,m}(t)$$
(6)

where \boldsymbol{g}_m is the mth column of \boldsymbol{G} , $\tau_{p,k} = \frac{2(R_k + r_{\text{IA}} - v_k p T_{\text{PRI}})}{c}$ is the round-trip time delay associated with the kth target, c is the speed of light and $\tilde{n}_{p,m}(t)$ is the additive Gaussian noise. For notational simplicity, we define $\tau_k \triangleq \frac{2R_k}{c}$, $\nu_k \triangleq \frac{2v_k f_c}{c}$ and

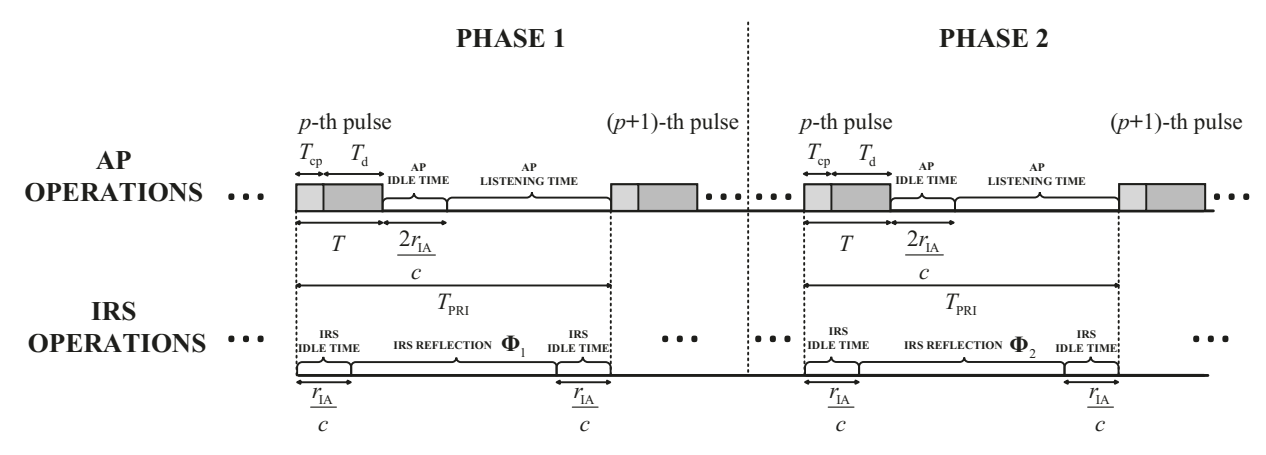


Fig. 3: A schematic of signal transmission for the two-phase NLOS sensing scheme.

 $au_0 \triangleq rac{2r_{ ext{IA}}}{c}$. We have $au_{p,k} = au_k + au_0 - rac{
u_k p T_{ ext{PRI}}}{f_c}$. After removing the carrier frequency, the baseband signal can be written as

$$\bar{y}_{p,m}(t) = \sum_{k=1}^{K} \bar{\alpha}_k b_m(\theta_k) z_p(\theta_k, \nu_k) s_p(t - \tau_{p,k}) + \bar{n}_{p,m}(t)$$
 (7)

where $\bar{\alpha}_k \triangleq \sqrt{P_t} \tilde{\alpha}_k e^{-j2\pi f_c(\tau_k + \tau_0)}$, $b_m(\theta_k) \triangleq \boldsymbol{g}_m^T \boldsymbol{\Phi}^T \boldsymbol{a}(\theta_k)$, $z_p(\theta_k, \nu_k) \triangleq \boldsymbol{a}^T(\theta_k) \boldsymbol{\Phi} \boldsymbol{G} \boldsymbol{w}_p e^{j2\pi pT_{\text{PRI}}\nu_k}$ and $\bar{n}_{p,m}(t)$ is the baseband noise.

Taking the Fourier transform of the received pth pulse baseband signal over the interval $[2r_{IA}/c+T+T_{cp}, 2r_{IA}/c+2T]$ (note that $\tau_0 = 2r_{\rm IA}/c$), the signal associated with the lth subcarrier is given by

$$\tilde{y}_{p,m}[l] = \int_{pT_{\rm PRI} + \tau_0 + TT}^{pT_{\rm PRI} + \tau_0 + 2T} \bar{y}_{p,m}(t) e^{-j2\pi l \Delta f t} \, dt \qquad (8)$$
 Plugging (4) and (7) into (8) and after some simplifying

operations, we have

$$\tilde{y}_{p,m}[l] = \beta T_{d} \sum_{k=1}^{K} \bar{\alpha}_{k} b_{m}(\theta_{k})$$

$$\times z_{p}(\theta_{k}, \nu_{k}) e^{-j2\pi l \Delta f(\tau_{k} + \tau_{0})} + n_{p,m}[l]$$
(9)

It is assumed that $n_{p,m}[l]$ is a complex Gaussian variable with zero mean and variance σ^2 , i.e., $n_{p,m}[l] \sim \mathcal{CN}(0,\sigma^2)$. Define $\alpha_k \triangleq \bar{\alpha}_k \beta T_d$, and ignore the common phase term τ_0 in (9), we have

$$y_{p,m}[l] = \sum_{k=1}^{K} \alpha_k b_m(\theta_k) z_p(\theta_k, \nu_k) e^{-j2\pi l \Delta f \tau_k} + n_{p,m}[l]$$
 (10)

Our objective in this paper is to estimate the DOAs, time delays and Doppler shifts associated with the K targets $\{\theta_k, \tau_k, \nu_k\}$. To this objective, we develop a two-phase sensing scheme, which allows us to construct two tensors and then a CPD-based method can be employed to jointly estimate the parameters even under the challenging scenario with $rank(\boldsymbol{G}) = 1.$

III. PROPOSED METHOD

A. Two-Phase Sensing Scheme

To resolve the inherent scaling ambiguity in target estimation, we consider a two-phase sensing scheme, in which the entire sensing cycle is divided into two phases, say, phase 1 and phase 2, and each of them is assigned a distinct IRS phaseshift profile. In each phase, the AP transmits P pulses in total. The pulse repetition interval is T_{PRI} , and the interval between the Pth pulse in phase 1 and the first pulse in phase 2 is also set to T_{PRI} (see Fig.3).

B. Tensor Representation and CPD

Let Φ_1 and Φ_2 denote the IRS phase shift matrices employed in phase 1 and phase 2, respectively. Define $b_{i,m}(\theta_k) \triangleq$ $\boldsymbol{g}_{m}^{T} \boldsymbol{\Phi}_{i}^{T} \boldsymbol{a}(\theta_{k}), \quad z_{i,p}(\theta_{k}, \nu_{k}) \quad \triangleq \quad \boldsymbol{a}^{T}(\theta_{k}) \boldsymbol{\Phi}_{i} \boldsymbol{G} \boldsymbol{w}_{p} e^{j2\pi p T_{\text{PRI}} \nu_{k}},$ where $i \in \{1, 2\}$. For each subcarrier l of the received echo signal in phase i, stacking the signal from all P pulses and all M antennas, we can construct a matrix $\mathbf{Y}_i(l) \in \mathbb{C}^{P \times M}$, with its (p, m)th entry denoted by (cf.(10))

$$y_{p,m}^{i}[l] = \sum_{k=1}^{K} \alpha_k b_{i,m}(\theta_k)$$

$$\times z_{i,p}(\theta_k, \nu_k) e^{-j2\pi l \Delta f \tau_k} + n_{i,p,m}[l]$$
(11)

Consequently, we have

$$\boldsymbol{Y}_{i}(l) = \sum_{k=1}^{K} \alpha_{k} f_{l}(\tau_{k}) \boldsymbol{z}_{i}(\theta_{k}, \nu_{k}) \boldsymbol{b}_{i}^{H}(\theta_{k}) + \boldsymbol{N}_{i,l}$$
(12)

where $z_i(\theta_k, \nu_k) \triangleq [z_{i,1}(\theta_k, \nu_k) \cdots z_{i,P}(\theta_k, \nu_k)]^T \in \mathbb{C}^P$, $b_i(\theta_k) \triangleq [b_{i,1}(\theta_k) \cdots b_{i,M}(\theta_k)] \in \mathbb{C}^M$, and $f_l(\tau_k) \triangleq e^{-j2\pi l\Delta f\tau_k}$. By concatenating the received signals across L subcarriers, we can naturally obtain a third-order tensor $\mathbf{\mathcal{Y}}_i \in \mathbb{C}^{P \times M \times L}$, with its (p, m, l)th entry given by $[\mathbf{Y}_i(l)]_{p,m}$, whose three modes respectively stand for the pulses, the AP's antennas, and the subcarriers. Note that each slice of the tensor \mathbf{y}_i is $\mathbf{Y}_i(l)$, which is a weighted sum of a common set of rankone outer products. Therefore the tensor ${oldsymbol{\mathcal{Y}}}_i$ admits a CPD as

$$\mathbf{\mathcal{Y}}_{i} = \sum_{k=1}^{K} \mathbf{z}_{i}(\theta_{k}, \nu_{k}) \circ \mathbf{b}_{i}(\theta_{k}) \circ \alpha_{k} \mathbf{f}(\tau_{k}) + \mathbf{\mathcal{N}}_{i}$$
(13)

where $f(\tau_k) \triangleq [e^{-j2\pi\Delta f \tau_k} \cdots e^{-j2\pi L\Delta f \tau_k}]^T$, $b_i(\theta) =$ $G^T \Phi_i a(\theta)$, \mathcal{N}_i denotes the additive noise, and \circ denotes the outer product. $z_i(\theta, \nu) = (\boldsymbol{W}^T \boldsymbol{G}^T \boldsymbol{\Phi}_i \boldsymbol{a}(\theta)) \otimes$ $(\boldsymbol{d}(\nu))$, in which $\boldsymbol{d}(\nu) \triangleq [e^{j2\pi T_{\text{PRI}}\nu} \cdots e^{j2\pi PT_{\text{PRI}}\nu}]^{T'} \in \mathbb{C}^P$, $\boldsymbol{W} \triangleq [\boldsymbol{w}_1 \cdots \boldsymbol{w}_P] \in \mathbb{C}^{M \times P}$ and \circledast denotes the Hadamard product. The associated factor matrices can be given by $\boldsymbol{A}_i \triangleq [\boldsymbol{z}_i(\theta_1,\nu_1) \cdots \boldsymbol{z}_i(\theta_K,\nu_K)] \in \mathbb{C}^{P \times K}, \ \boldsymbol{B}_i \triangleq [\boldsymbol{b}_i(\theta_1) \cdots \boldsymbol{b}_i(\theta_K)] \in \mathbb{C}^{M \times K}, \ \boldsymbol{C} \triangleq [\alpha_1 \boldsymbol{f}(\tau_1) \cdots \alpha_K \boldsymbol{f}(\tau_K)] \in \mathbb{C}^{L \times K}$. Under a mild condition, the unique CPD of $\boldsymbol{\mathcal{Y}}_i$ can be achieved by utilizing the Vandermonde structure of the factor matrix \boldsymbol{C} [8].

C. Target Parameters Estimation

After CPD, we now have access to the estimated factor matrices $\{\hat{A}_i, \hat{B}_i, \hat{C}_i\}$, in which $i \in \{1, 2\}$. Note that for both phases, the factor matrix C_i remains the same, i.e. $C_1 = C_2 = C$. Due to the inherent permutation and scaling ambiguities, the estimated factor matrices are related with the true factor matrices as

$$\begin{cases}
\hat{A}_{1} = A_{1}\Lambda_{1}\Pi_{1} + E_{1} \\
\hat{B}_{1} = B_{1}\Lambda_{2}\Pi_{1} + E_{2} \\
\hat{C}_{1} = C\Lambda_{3}\Pi_{1} + E_{3}
\end{cases}
\begin{cases}
\hat{A}_{2} = A_{2}\Gamma_{1}\Pi_{2} + \tilde{E}_{1} \\
\hat{B}_{2} = B_{2}\Gamma_{2}\Pi_{2} + \tilde{E}_{2}
\end{cases} (14)$$

where $\{\Lambda_1, \Lambda_2, \Lambda_3, \}$ and $\{\Gamma_1, \Gamma_2, \Gamma_3, \}$ are unknown nonsingular diagonal matrices satisfying $\Lambda_1 \Lambda_2 \Lambda_3 = I$ and $\Gamma_1 \Gamma_2 \Gamma_3 = I$, $\{\Pi_i\}$ are unknown permutation matrices, $\{E_1, E_2, E_3\}$ and $\{\tilde{E}_1, \tilde{E}_2, \tilde{E}_3\}$ are estimation errors.

Notice that both \hat{C}_1 and \hat{C}_2 are associated with a common matrix C. This fact can be used to remove the relative permutation between \hat{C}_1 and \hat{C}_2 . Define

$$\rho_{k_1,k_2} = \frac{|(\hat{\boldsymbol{c}}_{1,k_1})^H \hat{\boldsymbol{c}}_{2,k_2}|}{\|\hat{\boldsymbol{c}}_{1,k_1}\|_2 \|\hat{\boldsymbol{c}}_{2,k_2}\|_2}$$
(15)

where \hat{c}_{1,k_1} and \hat{c}_{2,k_2} are, respectively, the k_1 th and k_2 th column of \hat{C}_1 and \hat{C}_2 . Since C has distinctive columns, with each column characterized by a different time delay parameter, ρ_{k_1,k_2} achieves the largest value when \hat{c}_{1,k_1} and \hat{c}_{2,k_2} correspond to the same target. Define a permutation matrix $\Pi_3 \triangleq [e_{\pi(1)} \cdots e_{\pi(K)}]^T \in \{0,1\}^{K \times K}$, where $e_{\pi(k)}$ is a standard basis vector, and $\pi(k) = \arg\max_{k_2} \{\rho_{k,k_2}\}_{k_2=1}^K$. Ignoring estimation errors, we should have $\Pi_2 = \Pi_1\Pi_3$. Then we can utilize Π_3 to remove the permutation between $\{\hat{A}_1\}$ and $\{\hat{A}_2\}$, $\{\hat{B}_1\}$ and $\{\hat{B}_2\}$, $\{\hat{C}_1\}$ and $\{\hat{C}_2\}$. For example, let $\hat{B}_1 \triangleq \hat{B}_1\Pi_3$, We have

$$\tilde{B}_1 = B_1 \Lambda_2 \Pi_1 \Pi_3 + E_2 \Pi_3 = B_1 \Lambda_2 \Pi_2 + E_2 \Pi_3$$
 (16)

Then we have column-aligned \tilde{B}_1 and \hat{B}_2 , i.e., the same columns of each pair of two factor matrices are associated with the same target. Similarly, we can access to $\tilde{A}_1 = A_1\Lambda_1\Pi_2 + E_1\Pi_3$, $\tilde{C}_1 = C\Lambda_3\Pi_2 + E_3\Pi_3$. Note that both \tilde{C}_1 and \hat{C}_2 are estimated as a Vandermonde matrix based on the estimated generators. Hence theoretically we should have $\Gamma_3\Lambda_3^{-1} = I$.

Recall that $\boldsymbol{b}_i(\theta) = \boldsymbol{G}^T \boldsymbol{\Phi}_i \boldsymbol{a}(\theta)$. Hence we can write $\boldsymbol{B}_i = \boldsymbol{G}^T \boldsymbol{\Phi}_i \boldsymbol{\Xi}$, where $\boldsymbol{\Xi} \triangleq [\boldsymbol{a}(\theta_1) \cdots \boldsymbol{a}(\theta_K)] \in \mathbb{C}^{N \times K}$. Note when rank $(\boldsymbol{G}) = 1$, \boldsymbol{G} can be expressed as $\boldsymbol{G} = \sigma \boldsymbol{u} \boldsymbol{v}^T$. Consequently, we define a new vector $\hat{\boldsymbol{r}}_k^B \in \mathbb{C}^M$, in which the mth entry can be calculated by the element-wise division of $[\tilde{\boldsymbol{B}}_1]_{m,k}$ and $[\hat{\boldsymbol{B}}_2]_{m,k}$, i.e.,

$$[\hat{\boldsymbol{r}}_{k}^{B}]_{m} \triangleq \frac{[\tilde{\boldsymbol{B}}_{1}]_{m,k}}{[\hat{\boldsymbol{B}}_{2}]_{m,k}} = \frac{\boldsymbol{u}^{T}\boldsymbol{\Phi}_{1}\boldsymbol{a}(\theta_{k})[\boldsymbol{\Lambda}_{2}]_{k,k}}{\boldsymbol{u}^{T}\boldsymbol{\Phi}_{2}\boldsymbol{a}(\theta_{k})[\boldsymbol{\Gamma}_{2}]_{k,k}} + \epsilon_{m,k}$$
(17)

Recall each column of \boldsymbol{A}_i is given by $\boldsymbol{z}_i(\theta_k, \nu_k) = (\boldsymbol{W}^T \boldsymbol{G}^T \boldsymbol{\Phi}_i \boldsymbol{a}(\theta_k)) \circledast (\boldsymbol{d}(\nu_k))$. Define $\hat{\boldsymbol{r}}_k^A \triangleq [\tilde{\boldsymbol{A}}_1]_{p,k}/[\hat{\boldsymbol{A}}_2]_{p,k}$. We have

$$[\hat{\boldsymbol{r}}_{k}^{A}]_{p} \triangleq \frac{[\tilde{\boldsymbol{A}}_{1}]_{p,k}}{[\hat{\boldsymbol{A}}_{2}]_{p,k}} = \frac{\boldsymbol{u}^{T} \boldsymbol{\Phi}_{1} \boldsymbol{a}(\theta_{k}) [\boldsymbol{\Lambda}_{1}]_{k,k}}{\boldsymbol{u}^{T} \boldsymbol{\Phi}_{2} \boldsymbol{a}(\theta_{k}) [\boldsymbol{\Gamma}_{1}]_{k,k}} + \varepsilon_{p,k}$$
(18)

in which both $\epsilon_{m,k}$ and $\varepsilon_{p,k}$ are noise terms. To remove the amplitude ambiguities, we further define

$$\hat{\gamma}(\theta_{k}) \triangleq \frac{1}{M} \sum_{m=1}^{M} [\hat{\boldsymbol{r}}_{k}^{B}]_{m} \cdot \frac{1}{P} \sum_{p=1}^{P} [\hat{\boldsymbol{r}}_{k}^{A}]_{p}$$

$$\approx \frac{\boldsymbol{u}^{T} \boldsymbol{\Phi}_{1} \boldsymbol{a}(\theta_{k}) [\boldsymbol{\Lambda}_{2}]_{k,k}}{\boldsymbol{u}^{T} \boldsymbol{\Phi}_{2} \boldsymbol{a}(\theta_{k}) [\boldsymbol{\Gamma}_{2}]_{k,k}} \cdot \frac{\boldsymbol{u}^{T} \boldsymbol{\Phi}_{1} \boldsymbol{a}(\theta_{k}) [\boldsymbol{\Lambda}_{1}]_{k,k}}{\boldsymbol{u}^{T} \boldsymbol{\Phi}_{2} \boldsymbol{a}(\theta_{k}) [\boldsymbol{\Gamma}_{1}]_{k,k}}$$

$$\stackrel{(a)}{=} \left(\frac{\boldsymbol{u}^{T} \boldsymbol{\Phi}_{1} \boldsymbol{a}(\theta_{k})}{\boldsymbol{u}^{T} \boldsymbol{\Phi}_{2} \boldsymbol{a}(\theta_{k})} \right)^{2}$$

$$(19)$$

where (a) comes from the fact that $\Lambda_1 \Lambda_2 \Lambda_3 = I$, $\Gamma_1 \Gamma_2 \Gamma_3 = I$, and $[\Gamma_3]_{k,k} [\Lambda_3]_{k,k}^{-1} = 1$.

Next, based on the above relationship, we can estimate the target's DOA via the following criterion

$$\hat{\theta}_{k} = \underset{\theta}{\operatorname{arg \, min}} \quad \|\hat{\gamma}(\theta_{k}) - \gamma(\theta)\|_{2}^{2}$$
s.t.
$$\gamma(\theta) = \left(\frac{\boldsymbol{u}^{T} \boldsymbol{\Phi}_{1} \boldsymbol{a}(\theta)}{\boldsymbol{u}^{T} \boldsymbol{\Phi}_{2} \boldsymbol{a}(\theta)}\right)^{2}, \, \theta \in \mathcal{D}_{\theta}$$
(20)

where \mathcal{D}_{θ} is the feasible region of θ and the above problem can be easily solved by a one-dimensional search.

Note that the kth column of \boldsymbol{A}_i is characterized by both θ_k and ν_k . Specifically, the kth column of \boldsymbol{A}_i and the kth column of \boldsymbol{B}_i are related as $\boldsymbol{z}_i(\theta_k,\nu_k)=(\boldsymbol{W}^T\boldsymbol{b}_i(\theta_k))\circledast(\boldsymbol{d}(\nu_k)).$ After the DOA is estimated, define $\check{\boldsymbol{B}}_i=\boldsymbol{G}^T\boldsymbol{\Phi}_i\hat{\boldsymbol{\Xi}}\in\mathbb{C}^{M\times K}$ with $\hat{\boldsymbol{\Xi}}\triangleq[\boldsymbol{a}(\hat{\theta}_1)\cdots\boldsymbol{a}(\hat{\theta}_K)],$ and define $\check{\boldsymbol{A}}_i\in\mathbb{C}^{P\times K}$ with $[\check{\boldsymbol{A}}_1]_{p,k}=[\check{\boldsymbol{A}}_1]_{p,k}/[\boldsymbol{W}^T\check{\boldsymbol{B}}_1]_{p,k},\ [\check{\boldsymbol{A}}_2]_{p,k}=[\hat{\boldsymbol{A}}_2]_{p,k}/[\boldsymbol{W}^T\check{\boldsymbol{B}}_2]_{p,k}.$ Hence the Doppler shift can be estimated via a correlation-based scheme as

$$\hat{\nu}_{i,k} = \operatorname*{arg\,max}_{\nu_k} \frac{|\check{\boldsymbol{a}}_{i,k}^H \boldsymbol{d}(\nu_k)|}{\|\check{\boldsymbol{a}}_{i,k}\|_2 \|\boldsymbol{d}(\nu_k)\|_2}$$
(21)

where $\check{a}_{i,k}$ denotes the kth column of A_i . We then compute the average of the two estimates as the final estimate of the Doppler shift, i.e., $\hat{\nu}_k = (\hat{\nu}_{1,k} + \hat{\nu}_{2,k})/2$. The velocity estimate of the kth target can be calculated as $\hat{v}_k = \hat{\nu}_k c/2f_c$. The round-trip time delay $\{\hat{\tau}_{i,k}\}$ can be calculated from the estimated generators $\{\hat{t}_{i,k}\}$ as

$$\hat{\tau}_{i,k} = \frac{\arg(\hat{t}_{i,k})}{-2\pi\Delta f} \tag{22}$$

where $\arg(\hat{t}_{i,k})$ denotes the argument of the complex number $\hat{t}_{i,k}$. Similarly, we obtain $\hat{\tau}_k = (\hat{\tau}_{1,k} + \hat{\tau}_{2,k})/2$.

IV. SIMULATION RESULTS

In this section, we present numerical results to evaluate the estimation performance of the proposed method for NLOS target sensing. We examine a two-dimensional scenario, where the AP and the IRS are located at coordinates $\mathbf{p}_{\text{AP}} = [0,0]^T$ and $\mathbf{p}_{\text{IRS}} = [100,100]^T$ m, respectively. In our simulations, the system carrier frequency is set to $f_c = 60$ GHz. The length of an effective OFDM symbol is set to $T_{\text{d}} = 2\mu\text{s}$

and the length of the CP is set to $T_{\rm cp}=1\mu {\rm s}$ [9]. The pulse repetition interval is set to $T_{PRI} = 8\mu s$. The channel of the AP-IRS link is generated based on the geometric channel model with only a LOS path and the distance-dependent path loss as in [10]. In our experiments, we consider K=2targets, both located within the angular range of $[30^{\circ}, 45^{\circ}]$ with respect to the IRS. The coordinates of the targets are set as $p_1 = [533, -170]^T$ m and $p_2 = [541, -245]^T$ m. The targets' radial velocities with respect to the IRS are set to $v_1 = 16.66$ m/s and $v_2 = -22$ m/s, respectively. The targets' radar crosssection (RCS) is assumed to be one [6]. In our experiments, the beamforming vector \boldsymbol{w}_p is optimized to orient its beam toward the IRS, maximizing the received signal power. The reflection coefficients of the IRS are set different in two different phases in order to exploit the diversity of the IRS's illumination patterns. The received signal-to-noise ratio (SNR) is defined as SNR $\triangleq \|\mathbf{y} - \mathbf{N}\|_F^2 / \|\mathbf{N}\|_F^2$. All results are averaged over 10^3 Monte Carlo runs.

The performance is evaluated by the mean square error (MSE), e.g., $MSE(\zeta) = \frac{1}{K} \sum_{k=1}^{K} \mathbb{E}\left(\|\zeta_k - \hat{\zeta}_k\|_2^2\right)$, where $\hat{\zeta}$ denotes an estimate of the parameter $\hat{\zeta}$, which corresponds to one of the parameters $\{\theta, \tau, \nu\}$. The MSE of our proposed method as a function of the SNR is plotted in Fig. 4(a)-4(c). The CRB results for different sets of parameters are also included for comparison. From Fig. 4(a)-4(c), we see that as the SNR increases, our proposed method achieves an estimation accuracy that is close to the theoretical lower bound. This result validates the efficiency of the proposed method for NLOS target sensing. Additionally, from Fig. 4, it is seen that the proposed method provides accurate estimates of the target's parameters even in a relatively low SNR regime, say SNR = -5dB. Notably, for NLOS sensing task, the SNR is usually low due to the round-trip path loss and reflection loss. Hence the ability of extracting parameters reliably under a low SNR environment has a significant implication in practice. We also compare our proposed method with the MLE-based method [6]. For a fair comparison, the AP-IRS channel is assumed to be Rician fading, i.e., $G=\sqrt{\gamma/(1+\gamma)}G^{\rm LOS}+\sqrt{1/(1+\gamma)}G^{\rm NLOS}$, where the Rician factor is set to $\gamma = 5 dB$. We focus the comparison on a single static target and rank(G) = 5. The results showcased in Fig. 4(d) demonstrate that our proposed algorithm has a clear performance advantage over the MLE-based method [6]. This can be explained as follows. The method in [6] requires additional degrees of freedom provided by the AP-IRS channel to resolve scaling ambiguity in DOA estimation. In contrast, our proposed method removes the scaling ambiguity by leveraging IRS illumination diversity across two phases.

V. CONCLUSION

In this paper, we proposed a novel two-phase sensing scheme for NLOS sensing in an IRS-assisted wireless system. The AP transmits OFDM pulses and then perceives the targets based on the echoes from the AP-IRS-targets-IRS-AP link. A CPD-based method was introduced to recover the DOAs, Doppler shifts, and time delays of the targets distributed in

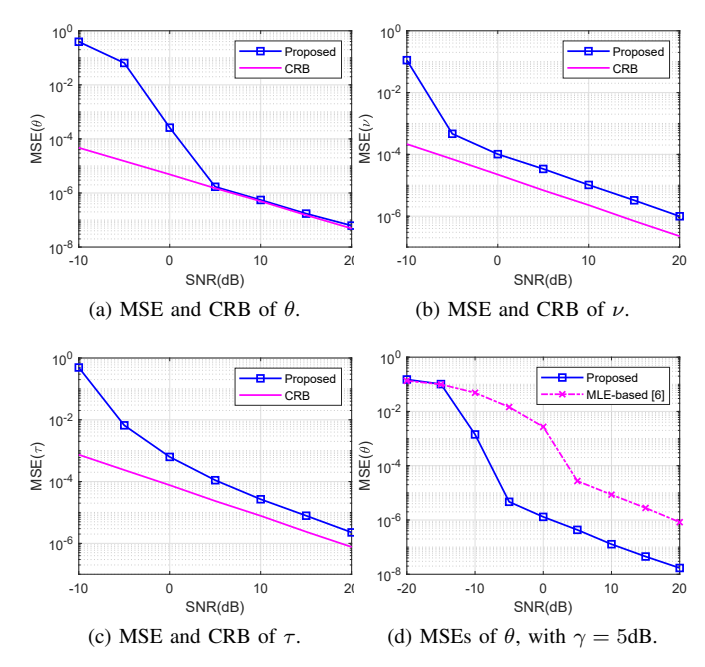


Fig. 4: MSEs/CRBs of target's parameters versus SNR, with P = 10, L = 10, M = 16, N = 32.

the NLOS region of the AP. Simulation results are provided to show the effectiveness of the proposed method.

REFERENCES

- [1] M. Di Renzo, A. Zappone, M. Debbah, M.-S. Alouini, C. Yuen, J. de Rosny, and S. Tretyakov, "Smart radio environments empowered by reconfigurable intelligent surfaces: How it works, state of research, and the road ahead," *IEEE Journal on Selected Areas in Communications*, vol. 38, no. 11, pp. 2450–2525, 2020.
- [2] Q. Wu, S. Zhang, B. Zheng, C. You, and R. Zhang, "Intelligent reflecting surface-aided wireless communications: A tutorial," *IEEE Transactions* on Communications, vol. 69, no. 5, pp. 3313–3351, 2021.
- [3] X. Shao, C. You, W. Ma, X. Chen, and R. Zhang, "Target sensing with intelligent reflecting surface: Architecture and performance," *IEEE Journal on Selected Areas in Communications*, vol. 40, no. 7, pp. 2070–2084, 2022.
- [4] A. Aubry, A. De Maio, and M. Rosamilia, "Reconfigurable intelligent surfaces for n-los radar surveillance," *IEEE Transactions on Vehicular Technology*, vol. 70, no. 10, pp. 10735–10749, 2021.
- [5] S. Buzzi, E. Grossi, M. Lops, and L. Venturino, "Foundations of mimo radar detection aided by reconfigurable intelligent surfaces," *IEEE Transactions on Signal Processing*, vol. 70, pp. 1749–1763, 2022.
- [6] X. Song, J. Xu, F. Liu, T. X. Han, and Y. C. Eldar, "Intelligent reflecting surface enabled sensing: Cramér-rao bound optimization," *IEEE Transactions on Signal Processing*, vol. 71, pp. 2011–2026, 2023.
- [7] C. R. Berger, B. Demissie, J. Heckenbach, P. Willett, and S. Zhou, "Signal processing for passive radar using ofdm waveforms," *IEEE Journal of Selected Topics in Signal Processing*, vol. 4, no. 1, pp. 226–238, 2010.
- [8] M. Sørensen and L. De Lathauwer, "Blind signal separation via tensor decomposition with vandermonde factor: Canonical polyadic decomposition," *IEEE Transactions on Signal Processing*, vol. 61, no. 22, pp. 5507–5519, 2013.
- [9] M. F. Keskin, V. Koivunen, and H. Wymeersch, "Limited feedforward waveform design for ofdm dual-functional radar-communications," *IEEE Transactions on Signal Processing*, vol. 69, pp. 2955–2970, 2021.
- [10] P. Wang, J. Fang, L. Dai, and H. Li, "Joint transceiver and large intelligent surface design for massive mimo mmwave systems," *IEEE Transactions on Wireless Communications*, vol. 20, no. 2, pp. 1052– 1064, 2021.